

Feasibility Assessment of New Hybrid Linear Motor Using Magnetostrictive Material

Jaehwan Kim, Jae-Kyun Doo and Jae-Do Kim

Dept. of mechanical engineering, Inha University, Incheon 402-751, South Korea

ABSTRACT

This paper deals with the feasibility assessment of hybrid linear motor that operates based on self-moving cell concept. The moving cell is composed of magnetostrictive actuator and a ring structure, and a cell train is constructed by connecting two cells in series. Since this motor uses strong push force of Terfenol-D actuators and friction force of the cells, it can essentially produce long stroke and large force. The overall performance of the motor was measured in terms of speed and force.

Keywords : Hybrid Linear Motor, Self-Moving Cell, Magnetostrictive Material—Terfenol-D

1. Introduction

Hybrid linear motors have been investigated for several decades since they have high thrust force related to their volume, high controllability and high position accuracy in the range of a few nano-meters. Comparing to conventional electromagnetic linear motors their mechanical structure is rather simple. They can generate direct linear movement without additional gear and spindle mechanisms^[1,2]. One of the most popular operation principle in the hybrid linear motors is inchworm motion. Inchworm type linear motor uses two clamping actuators and one pushing actuator^[3]. Combination of two clamping devices and one pushing actuator generates a “worm”-like motion. Inchworm type motor has the advantages of decoupling vibration system that generates elliptical motion on the stator surface to allow the greater efficiency over the wave type motion. However, holding force of the motor critically depends on the clamping actuator output. Usually clearance between the moving shaft and clamping device should be maintained in order for the motor to run smoothly. Since the deflection of the clamping actuator is so small that it is hard to keep the gap between the clamping device and the shaft. To cope with this problem, lever mechanisms with flexural hinges have been used such that the stroke

of piezoelectric actuator is increased^[4]. There is trade-off between the output force and the stroke: as the stroke increases, the output force is decreased.

Magnetostrictive materials have been recognized as giant strain materials compared with piezoelectric materials. Schemes using magnetostrictive materials as long stroke linear motors normally involve designs that rectify the tiny motions of the material to produce large displacements. One early concept was to tightly insert a Terfenol-D rod into a tube, using a magnetic field to compress the rod in a wave-like pattern so that it moves like an inchworm through the tube^[5]. This design relies on tight tolerance and makes the Terfenol-D rod the wear element in the motor, gradually worsening tolerances and wearing at the heart of the motor.

The inchworm linear motors have some difficulties in clamping and pushing functions. So we aim at improving the design and developing a new hybrid linear motor that is compact and promises better operational characteristics in terms of high force, high specific power, long stroke capability and high energy efficiency. Magnetostrictive material is used for the actuators of the motor.

2. Hybrid Linear Motor

2.1 Working Principle

The proposed motor operates based on self-moving

cell concept. The cell is composed of Terfenol-D linear actuator and a ring shaped shell (Fig. 1). A cell train is constructed by connecting two cells in series and fit in a guideway. The working principle is represented in Fig. 2.

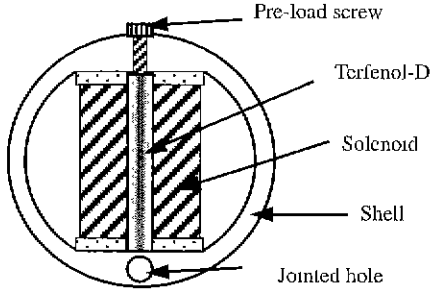


Fig. 1 Moving cell.

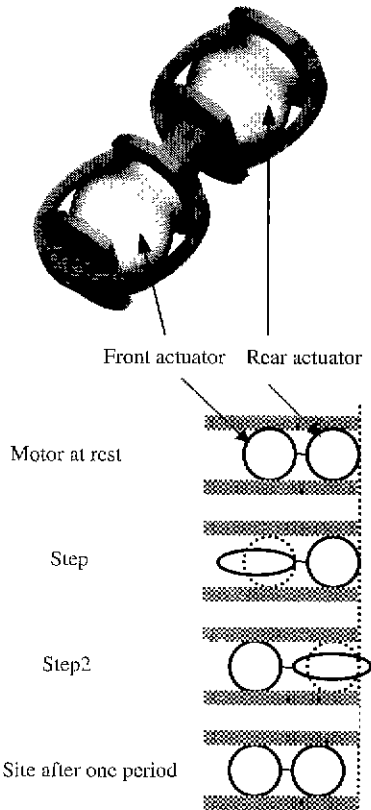


Fig. 2 Working principle.

Since the cells are fit into a straight guideway with interference, they are locked without any slippage in the absence of excitation on the actuators. When the Terfenol-D actuator in the front cell is activated the cell

stretches out such that it loses its clamping force and moves out along the axial direction. The moving distance is proportional to the displacement of the activated Terfenol-D actuator. Once each cell is energized in succession, a worm-like motion of the train of moving cells can be generated relative to the guideway. The speed of the moving cell train is proportional to the activation frequency and the amplitude of the excitation current. Terfenol-D rods are prestressed by the pre-load screws to increase the strain output. As a proof-of-concept stage, two cells are used. By increasing the number of cells, the movement of cell train can be smooth

The distinguished merit of the motor is that two operating modes are possible: speed and force modes. Fig. 3 illustrates the two operating modes with three moving cells. In the force mode, large clamping force can be obtained by adapting many clamping cells. In the speed mode, the displacement output can be increased by activating several neighboring cells, simultaneously.

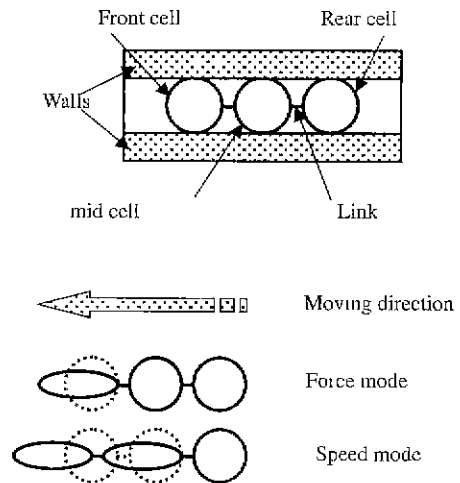


Fig. 3 Two operating modes: force and speed modes.

2.2 Moving Cell

Key issues of the moving cell is clamping force and moving velocity. The interference dimension should be enough to maintain the desired clamping force meanwhile the Terfenol-D actuator should be able to stretch out the shell structure such that the clamping force is mutilated. Thus, the configuration of shell is very important in the clamping force and the moving velocity.

The shell is basically a ring where a part of inside is trimmed in parallel so that the Terfenol-D rod ($\phi 6 \times 50$ mm) and solenoid are securely mounted. The shell is made of brass that exhibits low magnetic flow leakage.

Finite element analysis is performed to investigate the deformation of the shell structure. Fig. 4 shows the deformed shape. When the clamping force in transverse direction is increased the transverse displacement is linearly increased and the average values of the shell stiffness were found to be 7725 N/mm for the shell structure (Table 1). This means that, for example, if 0.01 mm is over-dimensioned in the first prototype, 77.25 N of clamping force can be obtained.

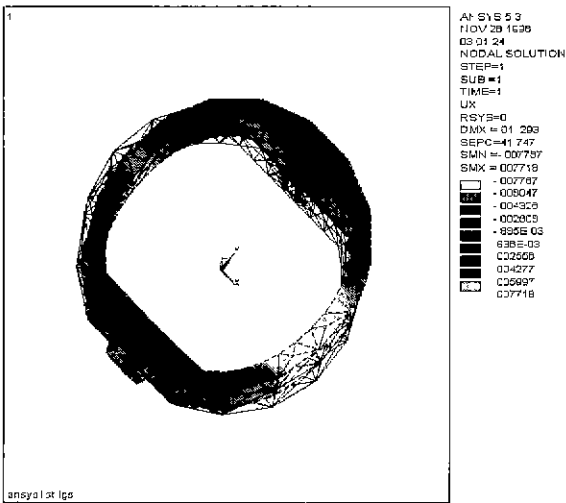


Fig. 4 Deformed shape of shell structure.

Table 1 Transverse stiffness of shell structure.

Load[N]	Maximum displacement [μm]	Stiffness [N/mm]
2	0.259	7722
20	2.589	7724.9
40	5.178	7724.9
60	7.767	7725
100	12.943	7726.2

2.3 Guideway

The guideway has two boundary walls and a bottom rail, which guides the cell train to travel. Since all external loads are finally supported by normal frictional forces between the walls and the shell structure of moving cell, the wall-shell interfaces should be designed

to have high friction coefficient with low wear rate. The surface of the two walls are ground and lapped to make the walls flat. Since the minimum stroke of the Terfenol-D actuators is the about 10 μm, the parallel tolerance of the two walls should be much smaller than the minimum stroke. The smaller tolerance is the better since some margin has to be saved for manufacturing tolerance, wear and the elastic deformation of shell structure. The wall is assembled to the bottom rail using three screws. This fastening mechanism results in nearly constant normal force between the walls and shells when the Terfenol-D actuators are activated.

When the cells are moving along the guideway the contact should be stable. The performance of the motor mainly depends on the quality of this contact mechanism and is affected by the normal friction force, the stiffness of the contact surface and the friction coefficient. It is recommended that the wall is rigid while the shell is relatively flexible so that the most deformation occurs at the shell.

3. Experiments

Two moving cells were manufactured and installed in the guideway after connecting them using a link (Fig. 5). Fig 6. represents the test setup. Personal computer generates the driving signals of half sine waves and the signals are fed into current amplifier (HP 6268B) in which current signals are produced according to the input signals. The current signals are applied to the solenoids in the moving cells to activate the Terfenol-D actuators. Current probe and proximeter (Bently Nevada) are used to measure the current and displacement, respectively. Prior to test the overall performance of the motor, individual cells are tested in terms of displacement output (Table 2). The displacement output of the front cell is nearly constant when the excitation frequency is changed while time delay is a little bit increased. Static friction force of cells were measured using weight and roller (Fig. 7). Table 3 shows the results. The static friction forces of front and rear cells are a little bit different due to the manufacturing tolerance. The minimum activation current means the current when the cell starts to move from the guideway. In other words, the moving cell should be activated above this current limit.

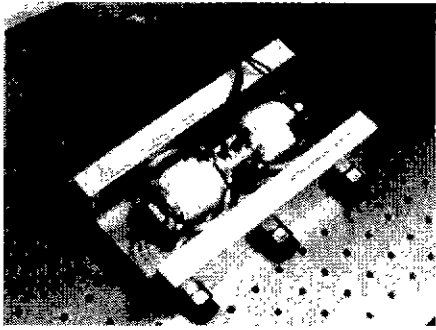


Fig. 5 Photograph of the hybrid linear motor.

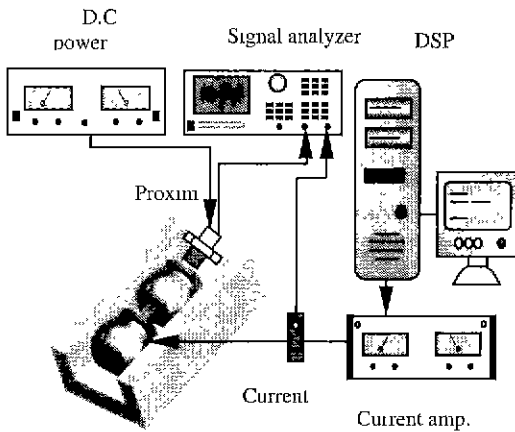


Fig. 6 Experimental setup for the motor performance measurement.

Table 2 Front cell performance.

Property Frequency	Time delay (msec)	Displacement (μm)
5Hz	9.3	22.62
10 Hz	15.2	23.08
15 Hz	15.6	22.34
20 Hz	16.1	22.2
25 Hz	16.6	21.6

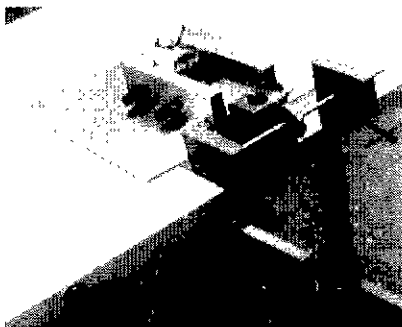
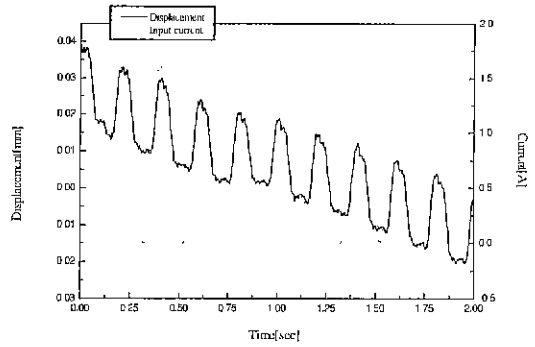


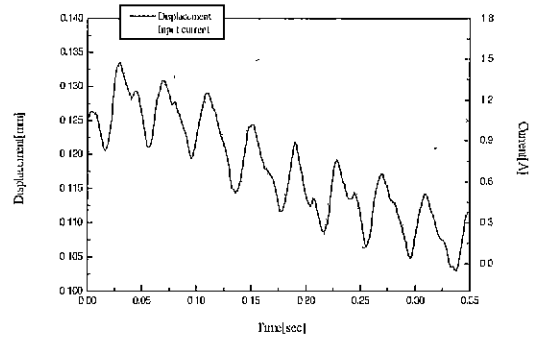
Fig. 7 Static friction measurement setup.

Table 3 Static friction force and min. activation current.

Actuator \ Property	Static-friction Force [N]	Minimum activation current [A]
Front	2.43	0.7
Rear	2.26	0.8



a. 5Hz



b. 25Hz

Fig. 8 Displacement and input current (1.6 A).

Fig. 8 represents the displacement output of the motor. Forwarding movement was found from the results when half sine current signal is applied. Nearly $5 \mu\text{m}$ resolution is achieved. The speed of the motor was measured according to different activation frequency and current (Fig. 9). As the frequency and current are increased, the speed is increased. Fig. 10 shows load-speed performance of the motor with different current. The current 1.2A is the minimum current that can move the motor. 2.5N of stall force and 0.045 mm/s of free speed are achieved under 2A current and 25Hz activation frequency. The stall force is closely related with the static friction force.

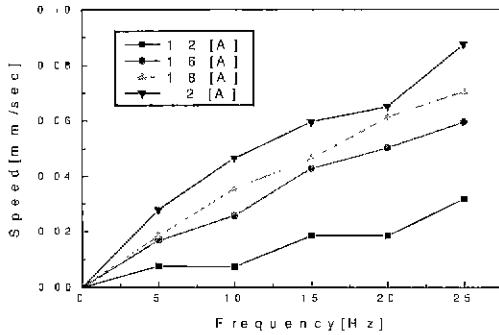


Fig. 9 Speed vs. frequency at various input current.

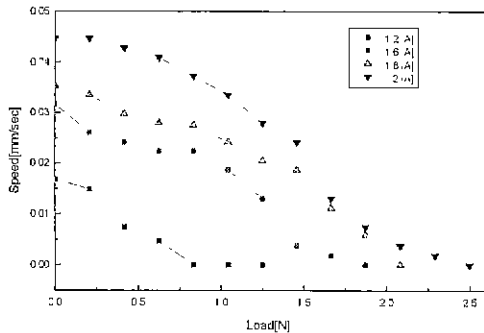


Fig. 10 Load characteristic of the motor (25 Hz).

4. Conclusions

The hybrid linear motor that operates based on self-moving cell concept was designed and tested. This motor basically can produce large force and long stroke. The overall performance of the motor was measured in terms of speed and force. The pushing force is directly related with the friction force of the cell. Since the cells are fit into the guideway with interference, fail-safe-lock is always guaranteed. By increasing the number of the cells and depending on the number of activating cells, two operating modes—speed mode and force mode can be achieved.

This new linear motor can be used for motion control, structural shape control, robot manipulator, position table and locomotion facility for advanced defense and civilian systems. This research is a proof-of-concept stage and more investigation in terms of number of cells, high frequency activation, wear and thermal effect should be followed.

Acknowledgement

This work was supported by the research grant (KRF-99-005-E00007) of KRF in Korea.

References

- Ikuta, K., Aritomi, S., and Kobashima, T., "Tiny Silent Linear Cybernetic Actuator Driven by Piezoelectric Device with Electromagnetic Clamp," *Proc. MEMS*, pp. 232-237, 1992.
- Seemann, W., "Ultrasonic travelling wave linear motor with improved efficiency." *Proc. of SPIE's Int. Symp. on Smart Structures and Materials*, Vol. 2717, pp. 554-560, 1996.
- Zhang, B., and Zhu, Z.Q., "Design of an inchworm type linear piezomotor," *Proc. of SPIE's Int. Symp. on Smart Structures and Materials*, Vol. 2190, pp. 528-539, 1994
- Xu, W., and King, T.G., "A new type of piezoelectric motor using a roller clutch mechanism," *Mechatronics*, Vol.6(3), pp. 303-315, 1996.
- Komttamasu, V., "Magnetostrictive Elastic Wave Type Linear Motion with TERFENOL-D," *Proc. of SPIE's Int. Symp. on Smart Structures and Materials*, Vol. 3044, pp. 363-369, 1997.